1   **Carbon monoxide (CO) cycling in the Fram Strait, Arctic Ocean**

2   **Hanna I. Campen*[1], Damian L. Arévalo-Martínez[1] and Hermann W. Bange[1]**

3   [1]Marine Biogeochemistry, GEOMAR Helmholtz Centre for Ocean Research Kiel, Düsternbrooker

4   Weg 20, 24105 Kiel, Germany

5   *corresponding author: Hanna I. Campen, hcampen@geomar.de

6   **Abstract**

7   Carbon monoxide (CO) influences the radiative budget and oxidative capacity of the atmosphere

8   over the Arctic Ocean, which is a source of atmospheric CO. Yet, oceanic CO cycling is

9   understudied in this area, particularly in view of the ongoing rapid environmental changes.

10   Therefore, incubation experiments were conducted in the Fram Strait in August/September 2019

11   under light, dark and pH-manipulated conditions. Lower pH did not affect CO cycling. Enhanced

12   CO production and consumption correlated with high absorption of colored dissolved organic

13   material and low dissolved nitrate concentrations, suggesting microbial CO uptake under

14   oligotrophic conditions which, in turn, controls the CO surface concentrations. Both production

15   and consumption of CO will likely increase in the future, but it is unknown which process will

16   dominate. Our results will help to improve models predicting future CO concentrations and

17   emissions and their effects on the radiative budget and the oxidative capacity of the Arctic

18   atmosphere.

19   **Plain Language Summary**

20   Carbon monoxide (CO) is a gas that affects the atmosphere in a similar way as a greenhouse gas.

21   It is is released from the ocean into the atmosphere. Because of that, it contributes to regional

22   warming in areas like the Arctic. However, not much is known about the main drivers of the CO

23   production and consumption processes in this area. Therefore, we conducted experiments in the

24   Fram Strait in August/September 2019 with surface water from four different locations and

25   investigated the effects of potential environmental changes such as acidification. The water

26   samples were exposed to light, darkness and acidified conditions for 48hrs. Acidification had no

27   influence, but we identified two environmental factors that may enhance CO production and

28   consumption: High amounts of organic material that absorbs UV light, and low concentrations of

29   nitrate, which is an essential nutrient fueling biological productivity in the ocean. CO consumption

30   and production may increase in the future, but more research is required to assess if one or the

31   other term will dominate. Our results will contribute to modelling studies to improve predictions

32   on the magnitude of Arctic CO release and its potential role in Arctic warming.

33   **1 Introduction**

34   Carbon monoxide (CO) is an atmospheric trace gas which plays an important role for the radiative

35   budget and oxidative capacity of the Earth's atmosphere (Forster et al., 2021).

36   Being ubiquitously supersaturated in the surface layer, the ocean is a source of CO to the

37   atmosphere (Conte et al., 2019). The global oceanic emissions of CO are a minor source

38   contributing only ~1% to the natural and anthropogenic sources of atmospheric CO. However, CO

39   has a comparably short atmospheric lifetime (~ 2 months). Thus, its oceanic emissions can

40   contribute significantly to the atmospheric budget, particularly in remote areas like the Arctic

41   Ocean being usually only marginally affected by direct anthropogenic CO emissions. The few

42   studies on CO in the Arctic Ocean report elevated and highly variable CO concentrations

43   compared to other ocean basins (Tran et al., 2013). The highest CO concentrations were observed

44   within bottom sea ice, suggesting production by ice algae (Song et al., 2011; Xie & Gosselin,

45   2005).

46

47   Oceanic CO is mainly produced photochemically via the reaction of UV-light with colored

48   dissolved organic matter (CDOM) and particulate organic matter (POM) (Song & Xie, 2017;

49   Stubbins et al., 2006). There is also evidence for biological CO production by phytoplankton (Gros

50   et al., 2009; McLeod et al., 2021; Tran et al., 2013) and for thermal (dark) CO production from

51   (C)DOM (Zhang et al., 2008). Tran et al. (2013) suggested that *Phaeocystis sp.*, dinoflagellates

52   and, to a lesser extent, diatoms are the major biological CO producers in the Fram Strait. However,

53   the CO production by algae lacks research on the physiological mechanisms and their

54   interdependencies with biogeochemical parameters (Campen et al., 2021). Beside the emissions

55   to the atmosphere, microbial consumption of CO is a major loss process in the ocean (Bates et al.,

56   1995; Conrad et al., 1982; Xie et al., 2005).

57   Ongoing environmental changes in the Arctic Ocean such as the loss of sea ice, changing light

58   penetration in the upper ocean, ocean acidification and altered nutrient and organic material supply

59   (e.g. Thackeray and Hall (2019); Hopwood et al. (2018); Stedmon et al. (2011); Terhaar et al.

60   (2020)), might affect CO production and consumption pathways as well as its emissions to the

61   atmosphere from this region (Campen et al., 2021). The distribution and magnitude of coastal

62   nutrient fluxes is predicted to change (e.g. Hopwood et al. (2018)) due to increasing freshwater

63   inputs via ice melting, which could lead to increased stratification, in turn limiting nutrient

64   remineralisation (Lannuzel et al., 2020). However, between 2012 and 2018 chlorophyll *a*

65   concentration in Arctic Ocean surface waters increased 16 times faster than before, suggesting an

66   additional input of nutrients that could even sustain an increase in primary production (Ardyna &

67   Arrigo, 2020) and with it CO precursors. Furthermore, light availability and penetration at the

68   ocean surface is projected to increase due to loss of ice and decreasing albedo (Castellani et al.,

69   2022; Pistone et al., 2014), potentially enhancing CO production in open surface waters and under-

70   ice water during the melting season. Due to the increase of atmospheric carbon dioxide (CO_2), the

71   pH in the surface ocean is decreasing (Canadell et al., 2021) and it was projected that the pH of

72   the Arctic Ocean surface waters could significantly decrease by the end of this century (Terhaar

73   et al., 2020). Decreasing pH (i.e. ocean acidification, OA) will alter biogeochemical cycles (Doney

74   et al., 2009). OA is likely to influence the CDOM pool which, in turn, would alter CO production

75   processes (Hopkins et al., 2020). However, to our knowledge, no studies on the effect of OA on

76   CO cycling in the ocean have been published (see Hopkins et al. (2020)).

77   Yet, the magnitude at which these environmental changes will affect CO production and emissions

78   from the Arctic Ocean is highly uncertain due to limited observations and lack of process

79   understanding. This study aims to elucidate the impact of ocean acidification, light changes and

80   multiple environmental parameters on CO consumption and production rates by means of in-situ

81   incubations conducted in the Fram Strait in 2019.

82   **2 Materials and Methods**

83   2.1 Study area

84   The study was conducted during the cruise JR18007 with RSS James Clark Ross to the Fram Strait

85   from 4 August to 6 September 2019. The Fram Strait, located between the west coast of Svalbard

86   and the east coast of Greenland, is characterized by the inflow of Atlantic water via the West

87   Spitzbergen Current (WSC) in the east and Arctic water outflow via the East Greenland Current

88   (EGC) in the west (e.g. Rudels et al. (2015)). Four incubation experiments were conducted at

89   stations NT6A, Ice2, D7 and D5 (see Fig. 1). The stations NT6A, Ice2 and D5 were located at the

90   shelf break. Ice 2 and D5 were also in proximity to the ice edge and D7 was located in the open

91   ocean region of the Fram Strait. The EGC affected Ice2 as indicated by its lower salinities and

92   colder water temperatures, whereas D7 and D5 were influenced by warmer and more saline

93   Atlantic waters of the WSC (see Table S1in the Supplement).
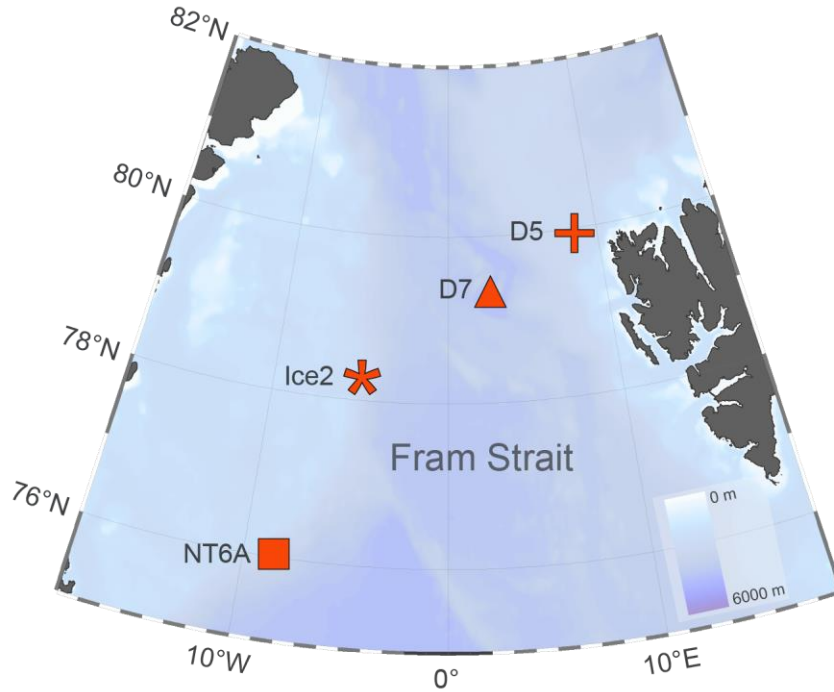
94

95   *Fig. 1 Map showing the locations where incubation experiments were performed (stations NT6A, Ice2, D7 and D5).*

96   2.2 Experimental set-up

97   For the incubation experiments, seawater from 5 m water depth was drawn from Niskin bottles

98   attached to a 12-bottle hydrocast-CTD/rosette and subsequently incubated in the experimental

99   enclosures for up to 48h. In total, eighteen 3.5 L light-transmitting incubation bottles (DURAN®,

100 borosilicate glass, GL 45, DWK Life Sciences, Germany) were filled with seawater. Lids (GL 45)

101 had PTFE-coated septa to easily press out the bulk water and close the bottles gas tightly. To

102 characterize the setting of the upper water a vertical profile down to 100 m was performed before

103 the start of the incubations. CO concentrations and ancillary measurements (see S2) from 5 m

104 water depth served as sampling time 0 (t_0) of the incubations.

105

106   Bubble-free seawater samples for the determination of dissolved CO were taken in triplicates in
107   100 mL glass vials (both from Niskin bottles and incubation bottles) with a Tygon® tubing to
108   avoid CO contamination by silicone rubber (Xie et al., 2002). The vials were immediately sealed
109   and stored between 0 and 6 °C in the dark to suppress further CO production in the light. CDOM
110   was sampled in brown glass vials of 500 mL with a screwed cap. Inorganic nitrate samples were
111   drawn into 10 mL polyethylene tubes, which were pre-rinsed three times with sample water, and
112   stored at -80° C until analysis at the GEOMAR's nutrient laboratory after the cruise. CDOM
113   samples were stored in the dark and below 5 °C until filtration (for method details see S2).

114   The pH in each experiment was manipulated to represent three different atmospheric CO_2 mole
115   fractions: 405.43 +/- 0.05 (Dlugokencky & Thoning, 2021), 670 and 936 ppm CO_2 for the
116   treatments named ambient, pH1 and pH2, respectively. To this end, the pH in pH1 and pH2, were
117   adjusted by -0.14 and -0.3, respectively, to approximate the IPCC's representative concentration
118   pathway (RCP) 4.5 (moderate change) and RCP 8.5 (extreme change) relative to the ambient
119   carbonate chemistry of the seawater at the time of the sampling. To manipulate the carbonate
120   system, $NaHCO_3$ and HCl were added (Riebesell et al., 2011) and immediately checked for the
121   resulting total alkalinity (TA) and dissolved inorganic (DIC) concentrations. Values of pCO_2 and
122   pH_T (total scale) were calculated with the software CO2sys (Lewis & Wallace, 1998). Immediately
123   after pH manipulation, bottles were gas tightly closed and incubated.

124   Light incubators had transparent Plexiglas sidewalls (GS 2458 UV transmitting) and no lid, so that
125   the full natural sunlight spectrum could penetrate the enclosed incubation bottles from the sides
126   and above (self-manufactured according to experimental needs, Fig. S3.1 in the supplements).
127   While these incubators were placed on deck to allow natural sunlight penetration, black and
128   covered water chambers served as dark incubators to exclude any light. All incubators were
129   continuously flushed with ambient seawater to keep bottles at ambient temperature. Light and
130   temperature were monitored continuously in each incubator (HOBO pendant® temperature/light,
131   onset, USA). Oxygen saturation was monitored (in %) to make sure that the incubations did not
132   become anoxic (O2xyDot®, OxySense, USA). CO concentrations were determined at the
133   beginning of the incubation (t_0), after 12 h (t_{12}), 24 h (t_{24}) and 48 h (t_{48}) of incubation (Fig. S3.1).

134   2.3 CO measurements

135   Dissolved CO concentrations were determined by the headspace method as described by Xie et al.

136   (2002). We established a headspace by injecting 15 mL CO-free synthetic air (purified via

137   MicroTorr series, 906 media, SAES group, USA). The samples were then equilibrated for eight

138   minutes. (Law et al., 2002; Xiaolan et al., 2010). A 5 mL subsample from the equilibrated

139   headspace was injected with a gastight syringe into the sample loop of a CO analyser (ta3000

140   AMETEK, USA). Every sixth sample injection was followed by the injection of a standard gas

141   mixture of 113.9 ppb CO in synthetic air (DEUSTE Gas Solutions, Germany) which was

142   calibrated against a certified standard gas (250.5 ppb CO, calibrated against the NOAA 2004 scale

143   at the Max Plank Institute for Biogeochemistry Jena, Germany).

144   Measured CO mole fractions from the headspace were corrected for the drift of the detector with

145   the standard gas measurements and corrected for water vapour (Wiesenburg & Guinasso, 1979).

146   The final dissolved CO concentrations were calculated based on Stubbins et al. (2006) with the

147   solubility coefficients from Wiesenburg and Guinasso (1979).

148   For each of the CO concentration triplicates we calculated the arithmetic mean and estimated the

149   standard error according to (David, 1951). The overall mean error for the measurements of

150   dissolved CO was +/- 0.025 nmol L^{-1} (+/- 17.4 %).

151   2.4 CO consumption and production rates

152   Net CO consumption (CR_{CO}) and production rates (PR_{CO}) were calculated as the slope of the linear

153   regression line through all sampling times for each (dark/light) experiment and each pH

154   (dark/light) treatment via a simple regression analysis. Gross production rates of CO (GP_{CO}) were

155   calculated as the difference between PR_{CO} and CR_{CO} in order to demask the effect of microbial

156   CO consumption.

157   Single CO gross production rates (singleGP_{CO}) were calculated between two sampling times (0 –

158   12 h, 0 – 24 h, 0 – 48 h) for each treatment and for each experiment, respectively to increase data

159   points when possible. To check whether the consumption rates follow a first order loss they were

160   plotted against the initial CO concentrations at t_0, $[CO]t_0$, of each incubation. All incubations

161   showed a first order loss (Fig. S3.2) and the consumption rate constant (k_{CO}) for each experiment

162   was thus determined as the slope of the linear regression.

163   **3 Results and Discussion**

164   3.1 CO concentration development during dark and light incubations

165   Fig. 2 gives an overview on how the CO concentrations ([CO]) developed over the incubation

166   duration of 48 hours: In all dark incubations, except for pH2 at NT6A , CO concentrations

167   decreased with time (i.e. over 48h). This was most likely resulted from microbial consumption of

168   CO which is the dominating CO consumption process in Arctic waters (e.g. Xie et al. (2009); Xie
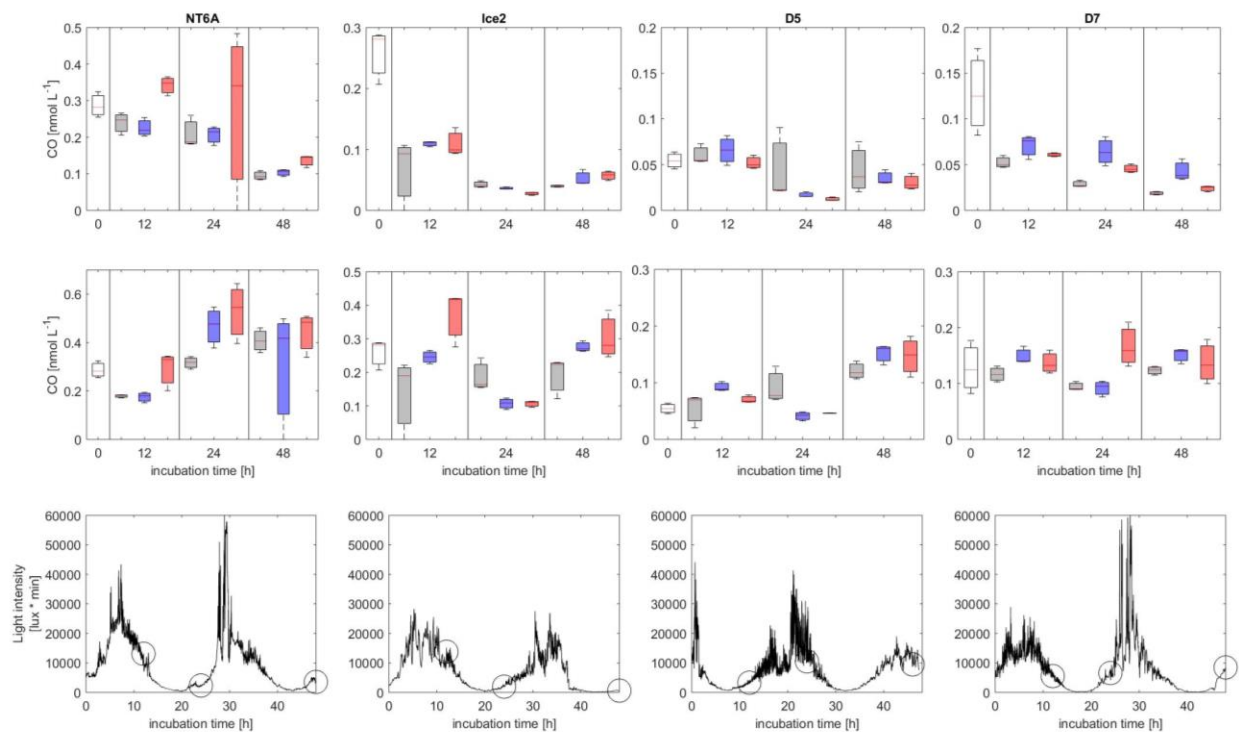
169   et al. (2005)).

170

171   *Fig. 2 Development of CO concentration (nmol L^{-1}) over 48 hours of incubations a) in the dark and b) in natural*

172   *sunlight. c) shows the respective light intensities in the light treatments at each station (light intensities in the dark*

173   *treatment were zero). Circles indicate the timing of sampling events in dark and light treatments.*

174   *white = initial concentration, grey = ambient, blue = pH1, red = pH2. The station names are indicated on the top.*

175   *Please note that the scales of the y axes are varying between stations according to their CO maximum concentrations.*

176

177   NT6A was an exception: pH2 showed an increase in [CO] in the dark after 12 and 24 h of 0.54

178   (+/- 7.9%) and 0.122 nmol L^{-1} (+/- 24.6 %) respectively. This increase could hint towards ongoing

179   thermal CO production (Zhang et al., 2008).

180   The low initial CO concentrations (Table 1) are in line with the observation that CO surface

181   concentrations can show a pronounced seasonal variability in Arctic waters. For example, Xie et

182   al. (2009) reported considerably lower CO concentrations for September/October 2003 (0.17 –

183   1.34 nmol L^{-1}) than for June 2004 (0.98 – 13 nmol L^{-1}) from the Amundsen Gulf in the Beaufort

184   Sea.

185   All light treatments showed a diurnal pattern of light intensity, though light was never completely

186   absent because the incubations were performed in the Arctic summer. CO concentrations in the

187   light incubations showed no uniform trend with time. Only during the incubations NT6A and D5

188   a significant increase of CO concentrations over 48h was observed. However, this is net

189   production which includes microbial CO consumption. Since there was no obvious relationship

190   between the timing of the sampling, [CO] and preceeding light intensities (Fig. 2), this indicates

191   that photochemical CO production did not exceed CO consumption. We speculate that if there was

192   photochemical CO production it was directly consumed by bacteria. Alternatively, biological CO

193   production by phytoplankton (Gros et al., 2009; Tran et al., 2013) or bacterioplankton and/or

194   thermal production might have been dominant at NT6A and D5 (Zhang et al., 2008).

195

196   Table 1: Initial CO concentrations and CO consumption rate constants (k_{CO}) of the four incubation

197   experiments conducted at different pH levels. Data are given as mean +/- estimate of standard

198   deviation (for the initial CO concentrations) and as the slope of the linear regression +/- error of

199   the slope (for k_{co}).

Station	Initial CO conc. nmol L^{-1}	k_{CO}, amb hr^{-1}	k_{CO}, pH1 hr^{-1}	k_{CO}, pH2 hr^{-1}
NT6A	0.28 +/- 0.035	-0.023 +/- 0.004	-0.021 +/- 0.003	-0.016 +/- 0.012
Ice2	0.25 +/- 0.041	-0.038 +/- 0.015	-0.035 +/- 0.018	-0.034 +/- 0.023
D5	0.05 +/- 0.009	-0.006 +/- 0.003	-0.014 +/- 0.019	-0.016 +/- 0.021
D7	0.13 +/- 0.049	-0.038 +/- 0.0095	-0.021 +/- 0.005	-0.033 +/- 0.005

200   The k_{CO} computed from our experiments (Table 1) are comparable to previously published

201   findings from Arctic waters: Xie et al. (2005) reported first order consumption rates constants k_{CO}

202 of -0.040 ± -0.012 hr^{-1} and -0.020 ± -0.0060 hr^{-1} in the coastal and offshore Beaufort Sea,

203 respectively. (Please note that the k_{CO} were given as positive values in Xie et al. (2005)).

204 In general, a lower pH did not affect the CO concentrations neither in the dark incubations nor in

205 the light incubations, since the CO concentrations in the pH manipulated treatments did not differ

206 significantly from the ambient treatments (as indicated by the error bars in Fig 2). Accordingly,

207 pH affected neither k_{CO} nor GP$_{CO}$ significantly (Fig. S3.3).

208

209 3.2 Effect of environmental variability on CO consumption and production

210 The effects of CDOM absorption, nitrate and Chl *a* concentrations and water mass properties on

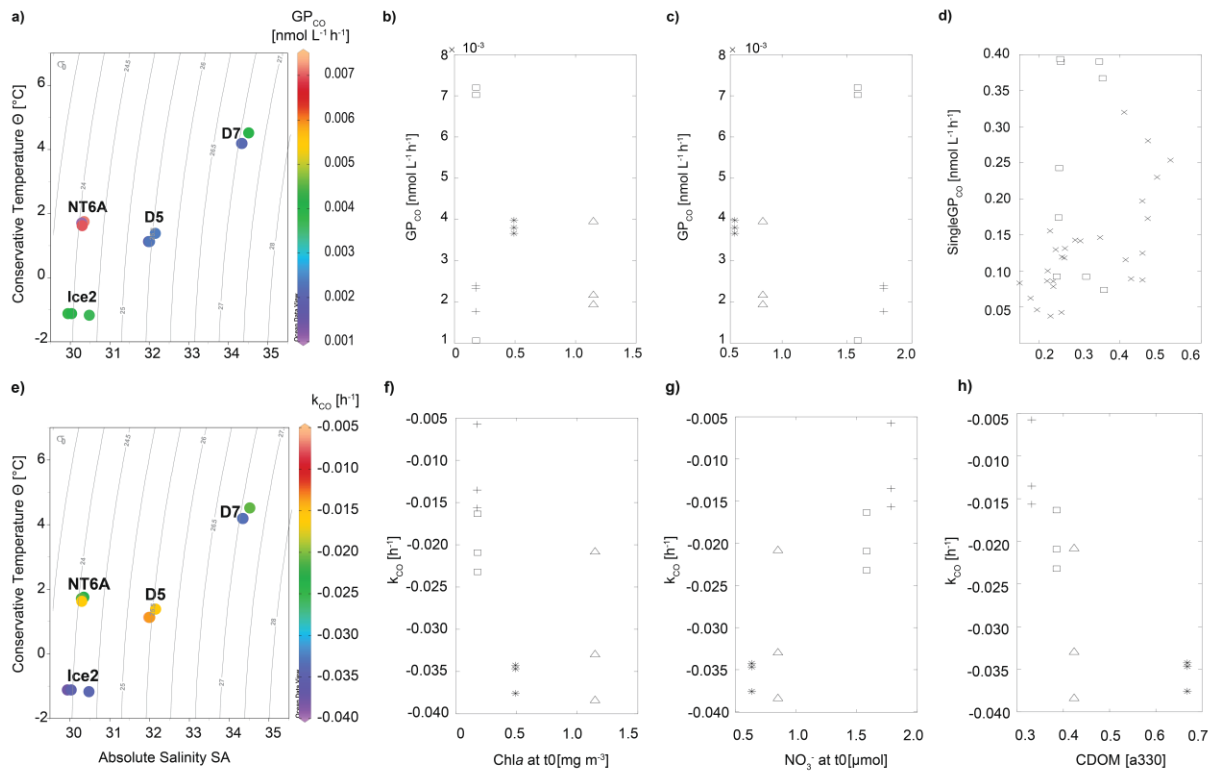211 the variability of k_{CO} and GP$_{CO}$ are shown in Fig. 3.

212

213

214 *Fig. 3 <u>Top row:</u> Relationship between GP$_{CO}$ and a) temperature/salinity incl. density, b) Chl a, c) NO$_3^-$ at t$_0$ and d)*

215 *relationship between singleGP$_{CO}$ and CDOM absorption (330 nm) at each sampling time.*

216 *<u>Bottom row</u>: Relationship between k$_{CO}$ and e) temperature/salinity incl. density, f) Chl a, g) NO$_3^-$ and h) CDOM*

217 *absorption (330 nm) at t$_0$. □ = NT6A, * = Ice2, + = D5, Δ = D7, x = CDOM values at single sampling times of all*

218 *stations excl. NT6A.*

219

220 3.2.1 Water mass properties

221 It is obvious that the stations Ice2 and D7 had contrasting hydrographic settings: While Ice2 was

222 located close to the ice edge and had a low water temperature and low salinity at t_0, D7 was located

223 in the open Fram Strait with a high water temperature and a higher salinity at t_0 (Fig. 3a). Therefore,

224 Ice2 was most probably affected by freshwater input from ice melting and polar waters carried by

225 EGC. D5 had a lower salinity compared to D7 and was also (at least partly) affected by freshwater

226 from ice melting. NT6A had a low salinity which was comparable to Ice2 but the water

227 temperature at t_0 was much higher compared to Ice2. Moreover, station NT6A had a steep

228 halocline in about 10 m, whereas Ice2 was well mixed in the upper layer (see depth profiles in

229 Supplements). Therefore, NT6A also being the southernmost station during our study had an

230 apparently different hydrographic setting in comparison to the other three stations. When ignoring

231 the data from NT6A, GPco showed a statistically significant correlation ($R^2 = 0.58$, $p < 0.05$) with

232 increasing density. This implies, that surface waters in the Fram Strait with a higher fraction of

233 freshwater (i.e. lower density), such as fresh meltwater or polar water characteristic for the EGC

234 in the west Fram Strait, potentially lead to higher CO production rates GPco. There was no

235 significant relationship for k_{CO} with density, which indicates that besides meltwater and polar

236 waters additional factors must be affecting k_{CO}.

237 3.2.2 CDOM

238 CDOM is an important driver for CO photoproduction in the Arctic Ocean (e.g. Song and Xie

239 (2017); Stubbins et al. (2006); Xie and Gosselin (2005)). However, CDOM absorption

240 significantly correlated with singleGP$_{CO}$ when the data from NT6A were excluded ($R^2 = 0.45$, p

241 < 0.05, Fig. 3c).

242 CDOM absorption at t_0 was significantly correlated with k_{CO} ($R^2 = 0.57$, $p < 0.05$, Fig. 3g). Given

243 that photochemical production from CDOM is a CO source, this is most likely an indirect

244 correlation: High CDOM absorption induces photochemical CO production which, in turn, results

245 in higher CO consumption (i.e. a lower k_{CO}), since k_{CO} depends on the initial CO concentration.

246 3.2.3 Chl *a*

247 Neither between Chl *a* and GP$_{CO}$ (Fig. 3b) nor between Chl *a* and k_{CO} a significant relationship

248 was found (Fig. 3f).

249   This is in contrast to Xie at al. [2005] who reported a negative correlation between Chl *a* and k_{CO}

250   (please note again that Xie et al. [2005] reported k_{CO} as positive values). This implies that Chl

251   *a*/k_{CO} relationships seems not to be uniform within the Arctic realm, pointing to regional

252   differences, possibly caused by the complex interplay between different water masses

253   (Cherkasheva et al., 2014; Rudels et al., 2015).

254   The combination of relatively higher Chl *a* concentrations at t_0 with lower nitrate concentrations

255   at Ice2 and D7 could explain the higher CO consumption rates at the two stations: nitrate might

256   be depleted by the present phytoplankton community so that microbes seem to use the produced

257   CO as an supplementary energy source (Cordero et al., 2019; Moran & Miller, 2007).

258   3.2.4 Nitrate

259   The effect of nitrate concentrations at t_0 on CO production rates was less obvious. There was a

260   negative trend (albeit statistically not significant at the 95% significance level) of GP_{CO} with NO_3^-

261   concentrations only when excluding the data from NT6A (Fig. 3c). Nitrate concentrations may

262   indirectly influence GP_{CO} rates. Enhanced GP_{co} rates at low NO_3^- concentrations may point to

263   stress-related CO production during increasing nitrogen limitation.

264   k_{CO} rates were positively correlated with nitrate concentrations at t_0 ($R^2 = 0.78$, $p<0.05$, Fig. 3f).

265   This correlation could result from CO consumption by microbes as a supplement energy source

266   when easily accessible nutrients like nitrate are depleted (Cordero et al., 2019).

267   **4 Conclusions**

268   In order to decipher the cycling of CO in the surface waters of the Fram Strait, we measured CO

269   production and consumption rates in various incubation experiments at four sites in the Fram Strait

270   in August/September 2019. Our results show that lower pH (representing future scenarios of ocean

271   acidification) did not affect CO gross production (GP_{CO}) and consumption (k_{CO}) rates. We

272   observed a tight coupling of CO production and consumption. Hence, the produced CO is not

273   necessarily emitted to the atmosphere as the dissolved CO seems to be rapidly consumed before

274   its atmospheric release. We conclude, therefore, that CO consumption mainly drives dissolved CO

275   concentrations and hence seems to act as filter for the subsequent atmospheric CO emissions from

276   the Fram Strait. This is line with the suggestion that microbial processes control the exchange of

277   CO across the ocean-atmosphere interface (Moran and Miller, 2007). High rates of both CO

278   production and CO consumption are favoured by a combination of high CDOM and low NO_3^-

279   concentrations. This points to a photochemical production of CO from CDOM which, in turn, is

280   consumed rapidly by microbes preferably under oligotrophic conditions (i.e. increasing nitrate

281   limitation). In the Arctic Ocean/Fram Strait, these conditions can be found both at ice edges as

282   well as in the open ocean where a supply of nutrients via melting and/or mixing is followed by

283   stratification (Cherkasheva et al., 2014). We identified both CDOM and nitrate as key drivers of

284   CO cycling. This has the implication that predicted changes in terrestrial-derived and marine

285   CDOM (e.g. Lannuzel et al., 2020), as well as dissolved nitrate inputs (Tuerena et al., 2022) will

286   likely affect future CO production and consumptionin the Fram Strait. Both trends might lead to

287   higher CO gross production as well as higher CO consumption. It is yet uncertain whether both

288   terms will balance each other out (as observed in our study) or whether one process will become

289   dominant. The question if and under which conditions k_{CO} would stagnate should be addressed in

290   future research, since in that situation CO would actually be emitted. Performing further

291   multifactorial experiments including i.e. UV light intensity and bacterial community data could

292   help to elucidate the explanatory power of the different environmental factors on both CO

293   production and consumption. This would facilitate a better incorporation of both terms into models

294   and would improve both CO emission estimates for the Arctic realm, and the assessment of how

295   atmospheric CO emissions will affect the radiative budget and oxidative capacity of the Arctic

296   atmosphere.

297   **Acknowledgements**

308

Author's Declaration

The authors declare no conflict of interests.

Open Research

Data Availability Statement

The data will be archived at the BODC database (https://www.bodc.ac.uk/data/all-data.html) by

the time of publication.

References

Ardyna, M., & Arrigo, K. R. (2020). Phytoplankton dynamics in a changing Arctic Ocean. *Nature Climate Change, 10*(10), 892-903. doi:10.1038/s41558-020-0905-y

Bates, T. S., Kelly, K. C., Johnson, J. E., & Gammon, R. H. (1995). Regional and seasonal variations in the flux of oceanic carbon monoxide to the atmosphere. *Journal of Geophysical Research: Atmospheres, 100*(D11), 23093-23101. doi:https://doi.org/10.1029/95JD02737

Campen, H. I., Arévalo-Martínez, D. L., Artioli, Y., Brown, I. J., Kitidis, V., Lessin, G., . . . Bange, H. W. (2021). The role of a changing Arctic Ocean and climate for the biogeochemical cycling of dimethyl sulphide and carbon monoxide. *Ambio*, 1-12. doi:10.1007/s13280-021-01612-z

Canadell, J. G., Monteiro, P. M., Costa, M. H., Cotrim da Cunha, L., Cox, P. M., Eliseev, A., . . . Koven, C. (2021). Global carbon and other biogeochemical cycles and feedbacks. *Climate change*.

Castellani, G., Veyssière, G., Karcher, M., Stroeve, J., Banas, S. N., Bouman, A. H., . . . Schourup-Kristensen, V. (2022). Shine a light: Under-ice light and its ecological implications in a changing Arctic Ocean. *Ambio, 51*(2), 307-317. doi:10.1007/s13280-021-01662-3

Cherkasheva, A., Bracher, A., Melsheimer, C., Köberle, C., Gerdes, R., Nöthig, E. M., . . . Boetius, A. (2014). Influence of the physical environment on polar phytoplankton blooms: A case study in the Fram Strait. *Journal of Marine Systems, 132*, 196-207. doi:https://doi.org/10.1016/j.jmarsys.2013.11.008

Conrad, R., Seiler, W., Bunse, G., & Giehl, H. (1982). Carbon monoxide in seawater (Atlantic Ocean). *Journal of Geophysical Research: Oceans, 87*(C11), 8839-8852.

Cordero, P. R., Bayly, K., Leung, P. M., Huang, C., Islam, Z. F., Schittenhelm, R. B., . . . Greening, C. (2019). Atmospheric carbon monoxide oxidation is a widespread mechanism supporting microbial survival. *The ISME Journal, 13*(11), 2868-2881.

David, H. (1951). Further applications of range to the analysis of variance. *Biometrika, 38*(3/4), 393-409.

Dlugokencky, E. J., J.W. Mund, A.M. Crotwell, M.J. Crotwell, and , & Thoning, K. W. (2021). Atmospheric Carbon Dioxide Dry Air Mole Fractions from the NOAA GML Carbon Cycle Cooperative Global Air Sampling Network. (1968-2020, Version: 2021-07-30). doi: https://doi.org/10.15138/wkgj-f215

343   Doney, S. C., Fabry, V. J., Feely, R. A., & Kleypas, J. A. (2009). Ocean acidification: the other CO2 problem. *Annual*
344   *review of marine science, 1*, 169-192.

345   Forster, P., Storelvmo, T., Armour, K., Collins, W., Dufresne, J.-L., Frame, D., . . . Watanabe, M. (2021). The Earth's
346   energy budget, climate feedbacks, and climate sensitivity.

347   Gros, V., Peeken, I., Bluhm, K., Zöllner, E., Sarda-Esteve, R., & Bonsang, B. (2009). Carbon monoxide emissions by
348   phytoplankton: evidence from laboratory experiments. *Environmental Chemistry, 6*(5), 369-379.
349   doi:https://doi.org/10.1071/EN09020

350   Hopkins, F. E., Suntharalingam, P., Gehlen, M., Andrews, O., Archer, S. D., Bopp, L., . . . Goris, N. (2020). The
351   impacts of ocean acidification on marine trace gases and the implications for atmospheric chemistry and
352   climate. *Proceedings of the Royal Society A, 476*(2237), 20190769.

353   Hopwood, M. J., Carroll, D., Browning, T., Meire, L., Mortensen, J., Krisch, S., & Achterberg, E. P. (2018). Non-
354   linear response of summertime marine productivity to increased meltwater discharge around Greenland.
355   *Nature communications, 9*(1), 1-9. doi:https://doi.org/10.1038/s41467-018-05488-8

356   Lannuzel, D., Tedesco, L., van Leeuwe, M., Campbell, K., Flores, H., Delille, B., . . . Wongpan, P. (2020). The future
357   of Arctic sea-ice biogeochemistry and ice-associated ecosystems. *Nature Climate Change, 10*(11), 983-992.
358   doi:10.1038/s41558-020-00940-4

359   Law, C. S., Sjoberg, T. N., & Ling, R. D. (2002). Atmospheric emission and cycling of carbonmonoxide in the Scheldt
360   Estuary. *Biogeochemistry, 59*(1), 69-94. doi:10.1023/A:1015592128779

361   Lewis, E., & Wallace, D. (1998). *Program developed for CO2 system calculations*. Retrieved from

362   McLeod, A. R., Brand, T., Campbell, C. N., Davidson, K., & Hatton, A. D. (2021). Ultraviolet Radiation Drives
363   Emission of Climate-Relevant Gases From Marine Phytoplankton. *Journal of Geophysical Research:*
364   *Biogeosciences, 126*(9), e2021JG006345. doi:https://doi.org/10.1029/2021JG006345

365   Moran, M. A., & Miller, W. L. (2007). Resourceful heterotrophs make the most of light in the coastal ocean. *Nature*
366   *Reviews Microbiology, 5*(10), 792-800.

367   Pistone, K., Eisenman, I., & Ramanathan, V. (2014). Observational determination of albedo decrease caused by
368   vanishing Arctic sea ice. *Proceedings of the National Academy of Sciences, 111*(9), 3322-3326.

369   Riebesell, U., Fabry, V. J., Hansson, L. W., & Gattuso, J. P. (2011). *Guide to best practices for ocean acidification*
370   *research and data reporting*.

371   Rudels, B., Korhonen, M., Schauer, U., Pisarev, S., Rabe, B., & Wisotzki, A. (2015). Circulation and transformation
372   of Atlantic water in the Eurasian Basin and the contribution of the Fram Strait inflow branch to the Arctic
373   Ocean heat budget. *Progress in Oceanography, 132*, 128-152.
374   doi:https://doi.org/10.1016/j.pocean.2014.04.003

375   Song, G., & Xie, H. (2017). Spectral efficiencies of carbon monoxide photoproduction from particulate and dissolved
376   organic matter in laboratory cultures of Arctic sea ice algae. *Marine Chemistry, 190*, 51-65.

377   Song, G., Xie, H., Aubry, C., Zhang, Y., Gosselin, M., Mundy, C., . . . Papakyriakou, T. N. (2011). Spatiotemporal
378   variations of dissolved organic carbon and carbon monoxide in first-year sea ice in the western Canadian
379   Arctic. *Journal of Geophysical Research: Oceans, 116*(C9).

380 Stedmon, C., Amon, R., Rinehart, A., & Walker, S. (2011). The supply and characteristics of colored dissolved
381   organic matter (CDOM) in the Arctic Ocean: Pan Arctic trends and differences. *Marine Chemistry, 124*(1-
382   4), 108-118.

383 Stubbins, A., Uher, G., Kitidis, V., Law, C. S., Upstill-Goddard, R. C., & Woodward, E. M. S. (2006). The open-
384   ocean source of atmospheric carbon monoxide. *Deep Sea Research Part II: Topical Studies in*
385   *Oceanography, 53*(14), 1685-1694. doi:https://doi.org/10.1016/j.dsr2.2006.05.010

386 Terhaar, J., Kwiatkowski, L., & Bopp, L. (2020). Emergent constraint on Arctic Ocean acidification in the twenty-
387   first century. *Nature, 582*(7812), 379-383. doi:10.1038/s41586-020-2360-3

388 Thackeray, C. W., & Hall, A. (2019). An emergent constraint on future Arctic sea-ice albedo feedback. *Nature*
389   *Climate Change, 9*(12), 972-978. doi:https://doi.org/10.1038/s41558-019-0619-1

390 Tran, S., Bonsang, B., Gros, V., Peeken, I., Sarda-Esteve, R., Bernhardt, A., & Belviso, S. (2013). A survey of carbon
391   monoxide and non-methane hydrocarbons in the Arctic Ocean during summer 2010. *Biogeosciences, 10*(3),
392   1909-1935.

393 Tuerena, R. E., Mahaffey, C., Henley, S. F., de la Vega, C., Norman, L., Brand, T., . . . März, C. (2022). Nutrient
394   pathways and their susceptibility to past and future change in the Eurasian Arctic Ocean. *Ambio, 51*(2), 355-
395   369. doi:10.1007/s13280-021-01673-0

396 Wiesenburg, D. A., & Guinasso, N. L. (1979). Equilibrium solubilities of methane, carbon monoxide, and hydrogen
397   in water and sea water. *Journal of chemical and engineering data, 24*(4), 356-360.

398 Xiaolan, L., Yang, G., Wang, X., Wang, W., & Ren, C. (2010). Determination of carbon monoxide in seawater by
399   headspace analysis. *Chinese Journal of Analytical Chemistry, 38*(3), 352-356.

400 Xie, H., Andrews, S. S., Martin, W. R., Miller, J., Ziolkowski, L., Taylor, C. D., & Zafiriou, O. C. (2002). Validated
401   methods for sampling and headspace analysis of carbon monoxide in seawater. *Marine Chemistry, 77*(2-3),
402   93-108.

403 Xie, H., Bélanger, S., Demers, S., Vincent, W. F., & Papakyriakou, T. N. (2009). Photobiogeochemical cycling of
404   carbon monoxide in the southeastern Beaufort Sea in spring and autumn. *Limnology and Oceanography,*
405   *54*(1), 234-249.

406 Xie, H., & Gosselin, M. (2005). Photoproduction of carbon monoxide in first-year sea ice in Franklin Bay,
407   southeastern Beaufort Sea. *Geophysical Research Letters, 32*(12).

408 Xie, H., Zafiriou, O. C., Umile, T. P., & Kieber, D. J. (2005). Biological consumption of carbon monoxide in Delaware
409   Bay, NW Atlantic and Beaufort Sea. *Marine Ecology Progress Series, 290*, 1-14.

410 Zhang, Y., Xie, H., Fichot, C. G., & Chen, G. (2008). Dark production of carbon monoxide (CO) from dissolved
411   organic matter in the St. Lawrence estuarine system: Implication for the global coastal and blue water CO
412   budgets. *Journal of Geophysical Research: Oceans, 113*(C12). doi:https://doi.org/10.1029/2008JC004811

413